A dual role of divalent metal ions in catalysis and folding of RNase H1 from extreme halophilic archaeon *Halobacterium* sp. NRC-1

Elias Tannous, Koji Yokoyama, Dong-Ju You [1], Yuichi Koga, Shigenori Kanaya *

Department of Material and Life Science, Graduate School of Engineering, Osaka University, 2-1 Yamadaoka, Suita, Osaka 565-0871, Japan

ABSTRACT

RNase H1 from extreme halophilic archaeon *Halobacterium* sp. NRC-1 (Halo-RNH1) consists of an N-terminal domain with unknown function and a C-terminal RNase H domain. It is characterized by the high content of acidic residues on the protein surface. The far- and near-UV CD spectra of Halo-RNH1 suggested that Halo-RNH1 assumes a partially folded structure in the absence of salt and divalent metal ions. It requires either salt or divalent metal ions for folding. However, thermal denaturation of Halo-RNH1 analyzed in the presence of salt and/or divalent metal ions by CD spectroscopy suggested that salt and divalent metal ions independently stabilize the protein and thereby facilitate folding. Divalent metal ions stabilize the protein probably by binding mainly to the active site and suppressing negative charge repulsions at this site. Salt stabilizes the protein probably by increasing hydrophobic interactions at the protein core and decreasing negative charge repulsions on the protein surface. Halo-RNH1 exhibited activity in the presence of divalent metal ions regardless of the presence or absence of 3 M NaCl. However, higher concentrations of divalent metal ions are required for activity in the absence of salt to facilitate folding. Thus, divalent metal ions play a dual role in catalysis and folding of Halo-RNH1. Construction of the Halo-RNH1 derivatives lacking an N- or C-terminal domain, followed by biochemical characterizations, indicated that an N-terminal domain is dispensable for stability, activity, folding, and substrate binding of Halo-RNH1.

© 2012 Federation of European Biochemical Societies. Published by Elsevier B.V. All rights reserved.

1. Introduction

RNase H (EC 3.1.26.4) is a universal enzyme that plays an essential role in cell growth and in maintaining the accuracy of the cell cycle [1–3]. It is also present in retroviruses as a C-terminal domain of reverse transcriptase (RT) and plays an essential role in viral proliferation [4]. The RNase H activity of human immunodeficiency virus (HIV) is therefore regarded as a target for AIDS therapy [5]. Being identified in all living organisms [6], RNase H shows several evolutionary modifications that enable it to tolerate the variety of environments in which its host organism grows, conserving its main function of cleaving the RNA strand of an RNA/DNA hybrid in an endonucleolytic manner [7]. Multiple RNases H are present in most organisms with low amino acid sequence similarity despite sharing a main chain fold and steric configuration of a DEDD

(Asp–Glu–Asp–Asp) or DEDE (Asp–Glu–Asp–Glu) active site motif [8]. Hence, they are classified into two major families: type 1 (RNase H1 and retroviral RNase H) and type 2 (RNases H2 and H3) RNases H [6,8]. RNase H cleaves the P-O3′ bond of RNA to produce 3′-OH and 5′-phosphate-ended products with a two-metal-ion catalysis mechanism [9–12]. For this mechanism to occur, RNase H utilizes two metal ions that will consecutively activate the nucleophile and promote the phosphoryl transfer reaction by destabilizing the enzyme–substrate complex.

Halobacterium sp. NRC-1 is an extreme halophilic archaeon that grows in a high-salt environment, maintaining an intracellular K^+ concentration of ∼4 M which is in turn equivalent to its extracellular Na^+ concentration [13]. Analyses of the genomes and proteomes of halophilic organisms indicate that proteins from these organisms are characterized by the high content of acidic residues, low content of basic residues, and low hydrophobicity [14]. These acidic residues compete with salt ions for free water and prevent the protein from aggregation in a high-salt condition, by forming a solvation shell that has a superior water binding capacity [15]. Structural and functional characterizations of proteins originating from halophilic organisms indicate that halophilic proteins require high concentration of salt for activity and stability, because negative-charge repulsions among acidic residues on the protein sur-

face decrease and stability of the core structure increases by the salting-out effect in a high-salt condition [16–24]. In a low-salt condition, these negative-charge repulsions prevent folding of proteins resulting in an inactive enzyme.

RNase H1 from *Halobacterium* sp. NRC-1 (Halo-RNH1) consists of an N-terminal domain (residues 1–68) with unknown function and a C-terminal RNase H domain (residues 69–199) [25]. In contrast to a representative member of non-halophilic RNases H1, *E. coli* RNase H1, which is a basic protein with the isoelectric point (p*I*) of 9.0 and shows the amino acid sequence identity of 33% to Halo-RNH1 [26], Halo-RNH1 is an acidic protein with the p*I* value of 4.2. Halo-RNH1 exhibits the highest enzymatic activity in the presence of 20 mM $MnCl_2$ or 100 mM $MgCl_2$. It retains at least 70% of the maximal activity in the presence of various concentrations of salt ranging from 0 to 2.5 M. Halo-RNH1 complements the temperature-sensitive growth phenotype of the mutant *E. coli* strain MIC2067 lacking all functional RNases H (RNases H1 and H2) [25]. These results suggest that Halo-RNH1 requires high concentration of salt for neither folding nor activity. However, it remains to be determined whether folding of Halo-RNH1 is independent of salt and whether substrate binding and stability of Halo-RNH1 are affected by salt. It also remains to be determined whether an N-terminal domain is important for activity and stability of Halo-RNH1.

In this study, we showed that Halo-RNH1 requires either salt or divalent metal ions for folding and is incompletely folded in the absence of both of them. Salt and divalent metal ions independently contribute to the stabilization of Halo-RNH1, suggesting that divalent metal ions play a dual role in catalysis and folding of Halo-RNH1. We also showed that the removal of an N-terminal domain does not seriously affect activity, stability, folding, and substrate binding of Halo-RNH1. Even though it has been shown that halophilic proteins require high concentration of salt for activity and stability [15–24], this is the first report on a dual role of divalent metal ions in catalysis and folding of halophilic proteins.

2. Material and methods

2.1. Plasmid construction

The pET25b derivatives for over-expression of the Halo-RNH1, Halo-CTD, and Halo-NTD genes were constructed by PCR. The genomic DNA of *Halobacterium* sp. NRC-1, which was kindly donated by Dr. M. Tokunaga, was used as a template. The sequences of the PCR primers are 5′-TGCAGCATATGCCAGTCGTCGAGTGCGACATCCAGACCGC-3′ for primer 1,5′-GCCGCGTCGAATTCCTTATCAGGCATCGTCGAGGGCC-3′ for primer 2,5′-TGCAGCATATGCGCGTGCACGCCTACTTCG-3′ for primer 3, and 5′-GCCGCGTCGAATTCCTTATCAGCCGCCGCGGTCGGGTTG-3′ for primer 4, where the NdeI (primers 1 and 3) and EcoRI (primers 2 and 4) sites are underlined. Primers 1 and 2, primers 2 and 3, and primers 1 and 4 were used to amplify the Halo-RNH1, Halo-CTD, and Halo-NTD genes, respectively. The resultant DNA fragments were digested with NdeI and EcoRI, and ligated into the NdeI-EcoRI sites of pET25b (Novagen).

All DNA oligomers for PCR were synthesized by Hokkaido System Science. PCR was performed with a GeneAmp PCR system 2400 (Applied Biosystems). The DNA sequences were confirmed by a Prism 310 DNA sequencer (Applied Biosystems).

2.2. Overproduction and purification

E. coli BL21-CodonPlus(DE3) (Stratagene) was used as a host strain to over-express the genes encoding Halo-RNH1 and its derivatives. The transformants of this strain with the pET25b derivatives were grown at 37 °C in LB medium containing 50 μg ml^{-1} ampicillin and 30 μg ml^{-1} chloramphenicol. When the absorbance at 600 nm reached approximately 0.5, 1 mM isopropyl thio-β-D-galactoside (IPTG) was added to the culture medium and cultivation was continued at 37 °C for an additional 4 h. The subsequent purification procedures of the recombinant proteins, which were different from those previously reported for Halo-RNH1 [25], were carried out at 4 °C. Cells were harvested by centrifugation at 8000*g* for 10 min, suspended in 10 mM Tris–HCl (pH 8.0) containing 1 mM EDTA (buffer A), lysed by sonication, and centrifuged at 30,000*g* for 30 min. The supernatant was collected, dialyzed against buffer A, and loaded onto a HiTrap Q HP column (5 ml) (GE Healthcare) equilibrated with the same buffer. The protein was eluted from the column with a linear gradient of NaCl from 0 to 1 M. The fractions containing the protein were collected, dialyzed against 5 mM sodium phosphate (pH 6.8), and applied to a hydroxyapatite column (5 ml) (BIO-RAD) equilibrated with the same buffer. The flow-through fraction was collected, dialyzed against 20 mM sodium acetate (pH 5.5) containing 1 mM EDTA and applied to a Mono Q column (1 ml) (GE Healthcare) equilibrated with the same buffer. The protein was eluted from the column with a linear gradient of NaCl from 0 to 1 M. The fractions containing the protein were collected and loaded to a HiLoad 16/60 Superdex 200pg column (GE Healthcare) equilibrated with buffer A. The fractions containing the protein were collected, dialyzed against 10 mM Tris–HCl (pH 8.0), and used for biochemical characterization. The purification procedures of Halo-NTD were slightly modified, such that the hydroxyapatite column chromatography step was eliminated. *E. coli* RNase H1 was overproduced and purified as previously described [27].

The purity of the protein was analyzed by Tricine SDS–PAGE (SDS–PAGE using the tricine buffer) using a 15% polyacrylamide gel [28], followed by staining with Coomassie Brilliant Blue (CBB). The protein concentration was determined from UV absorption using a cell with an optical path length of 1 cm and an A280 value for 0.1% (1.0 mg ml^{-1}) solution of 1.26 for Halo-RNH1, 1.39 for Halo-CTD, 0.99 for Halo-NTD, and 2.02 for *E. coli* RNase H1. These values, except for that of *E. coli* RNase H1 experimentally determined [29], were calculated by using absorption coefficients of 1576 M^{-1} cm^{-1} for Tyr and 5225 M^{-1} cm^{-1} for Trp at 280 nm [30].

2.3. CD spectra

The CD spectra were measured on a J-725 spectropolarimeter (Japan Spectroscopic) at 25 °C. The proteins were dissolved in 10 mM Tris–HCl (pH 8.0) containing various concentrations of NaCl, KCl, $MnCl_2$, $MgCl_2$, or $CaCl_2$. For measurement of the far-UV CD spectra (200–260 nm), the protein concentration was approximately 0.1 mg ml^{-1} and a cell with an optical path length of 2 mm was used. For measurement of the near-UV CD spectra (250–320 nm), the protein concentration was approximately 1.0 mg ml^{-1} and a cell with an optical path length of 10 mm was used. The mean residue ellipticity, θ, which has the units of deg cm^{-2} dmol^{-1}, was calculated by using an average amino acid molecular mass of 110 Da.

2.4. Thermal denaturation

Thermal denaturation of the proteins was analyzed by monitoring the change in CD values at 222 nm as the temperature was increased. The proteins were dissolved in 10 mM Tris–HCl (pH 8.0) containing 50 mM or 3 M NaCl, 20 mM $MnCl_2$, 300 mM $MgCl_2$, 3 M NaCl and 20 mM $MnCl_2$, or 3 M NaCl and 300 mM $MgCl_2$. The protein concentration and optical path length were 0.1 mg ml^{-1} and 2 mm, respectively. The temperature of the protein solution was linearly increased by approximately 1.0 °C/min. Thermal denaturation of the proteins was reversible at the conditions examined. The temperature of the midpoint of the transition, T_m, was calcu-

lated from curve fitting of the resultant CD values versus temperature data on the basis of a least squares analysis.

2.5. ANS fluorescence spectroscopy

Binding of 1-anilino-8-naphthalenesulfonic acid (ANS) (Wako) to the protein was analyzed by measuring the fluorescence of ANS at 20 °C. The protein (1 μM) and ANS (50 μM) were dissolved in 10 mM Tris–HCl (pH 8.0) in the presence or absence of 20 mM MnCl₂, 3 M NaCl, or 6 M GdnHCl. The fluorescence emission was monitored from 400 to 600 nm at an excitation wavelength of 380 nm using spectrofluorophotometer RF-5300PC (Shimadzu). The spectrum obtained in the absence of the protein was used as a blank.

2.6. Enzymatic activity

The RNase H activity was determined by using 12 bp RNA/DNA hybrid (R12/D12) as a substrate. This oligomeric substrate was prepared by hybridizing 1 μM of the 5′-(6-carboxyfluorescein)-labeled 12 base RNA (5′-cggagaugacgg-3′) with a 1.5 M equivalent of the complementary DNA as described previously [31]. Hydrolysis of the substrate at 37 °C for 15 min and separation of the products on a 20% polyacrylamide gel containing 7 M urea were carried out as described previously [31]. The reaction buffer was 10 mM Tris–HCl (pH 8.5) containing 1 mM DTT, 0.01% BSA, 50 mM or 3 M NaCl, and various concentrations of MgCl₂ or MnCl₂ for Halo-RNH1 and Halo-CTD, and 10 mM Tris–HCl (pH 8.0) containing 1 mM DTT, 0.01% BSA, 50 mM or 3 M NaCl, and 10 mM MgCl₂ for E. coli RNase H1. The substrate concentration was 1 μM for Halo-RNH1 and Halo-CTD, and 0.5 μM for E. coli RNase H1. The products were detected by Typhoon 9240 Imager (GE Healthcare) and quantified using Image Quant 5.2 analysis software. One unit is defined as the amount of enzyme degrading 1 μmol of the substrate per min at 37 °C. The specific activity was defined as the enzymatic activity per milligram of protein.

2.7. Binding analysis to substrate

Binding of the proteins to the substrate was analyzed in the absence of divalent metal ions using a Biacore X instrument (Biacore) as described previously [32]. The proteins were dissolved in 10 mM Tris–HCl (pH 8.0) containing 50 mM or 3 M NaCl, 1 mM EDTA, 1 mM β-Me, and 0.005% Tween P20 at various concentrations. The proteins were injected at 25 °C at a flow rate of 10 μl min⁻¹ onto the sensor chip on which the 29 bp RNA/DNA hybrid was immobilized. To determine the association constant, K_A, the concentration of the protein injected onto the sensor chip was varied in the range 20–800 nM for Halo-RNH1, 30–900 nM for Halo-CTD, and 3–50 μM for Halo-NTD. From the plot of the equilibrium binding responses as a function of the concentrations of the proteins, the K_A value was determined using the steady-state affinity software available in BIAEVALUATION (Biacore).

2.8. Homology modeling

A model for the three-dimensional structure of Halo-RNH1 without the N-terminal domain was built by SWISS-MODEL – automated protein homology-modeling server – (Swiss Institute of Bioinfomatics) [33], using the structure of the RNase H domain of the bifunctional protein Rv2228c from *Mycobacterium tuberculosis* (PDB ID: 3HST) [34] as a template. These proteins share the amino acid sequence identity of 45%. The model was viewed and edited with PyMOL (www.pymol.org). Calculations of the electrostatic surface potentials were performed by solving the Poisson–Boltzmann equation with PyMOL Adaptive Poisson–Boltzmann Solver (APBS) tools [35].

3. Results and discussion

3.1. Tertiary model of Halo-RNH1

Halobacterium sp. NRC-1 RNase H1 (Halo-RNH1) is characterized by the high content (17.5%) of acidic amino acid residues. A tertiary model of the RNase H domain of this protein shows the abundance of acidic residues on the surface, with some aspartate residues forming clusters (Fig. 1(A)). As a result, the surface of the RNase H domain of Halo-RNH1 is negatively charged (Fig. 1(B)). The overall structure of the RNase H domain of Halo-RNH1 is similar to that of *E. coli* RNase H1, except that it lacks a basic protrusion. The steric configurations of the four acidic active site residues (Asp75, Glu115, Asp139, and Asp189) are similar to those of *E. coli* RNase H1. Because at least a single divalent metal ion binds to the active site of *E. coli* RNase H1 even in the absence of the substrate [36–38], this metal ion may also bind to the active site of Halo-RNH1 even in the absence of the substrate.

3.2. Requirement of salt or divalent metal ions for folding of Halo-RNH1

To examine whether Halo-RNH1 requires salt or divalent metal ions for folding, the far-UV CD spectrum of Halo-RNH1 was measured in the presence or absence of various concentrations of NaCl (Fig. 2(A)), MnCl₂ (Fig. 2(B)), or MgCl₂ (Fig. 2(C)). In the absence of salt and divalent metal ions, the far-UV CD spectrum of Halo-RNH1 gives a trough with a minimum [θ] value of −13,000 at 205 nm, which is accompanied by a shoulder with a [θ] value of −8000 at 222 nm. However, this spectrum is considerably changed in the presence of salt or divalent metal ions so that the helical content of the protein increases. As a result, the far-UV CD spectrum of Halo-RNH1 gives a broad trough with a minimum [θ] value of approximately −13,000 at 222 nm in the presence of ≥2 M NaCl (Fig. 2(A)), ≥10 mM MnCl₂ (Fig. 2(B)), or ≥300 mM MgCl₂ (Fig. 2(C)). This spectrum was not significantly changed in the presence of both 2 M NaCl and 10 mM MnCl₂ or 300 mM MgCl₂ (data not shown). A similar spectrum was obtained in the presence
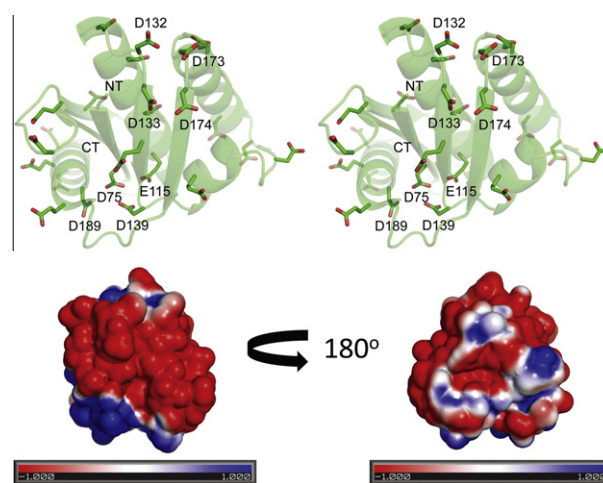

Fig. 1. A tertiary model of Halo-CTD. (A) Stereoview of the tertiary model of Halo-CTD. The side chains of the acidic residues on the surface, including four active site residues (D75, E115, D139, D189) and four residues appearing as a cluster (D132, D133, D173, D174), are shown as deep green stick models, in which the oxygen atoms are colored red. NT and CT represent N and C-termini. (B) Electrostatic surface potentials of Halo-CTD. The negative and positive potentials are in red and blue, respectively. The electrostatic potential value ranges from −1 to +1 kT/e. The view direction of the structure in the left panel, which is rotated by 180° in the right panel, is the same as in (A). (For interpretation of the references to color in this figure legend, the reader is referred to the web version of this article.)
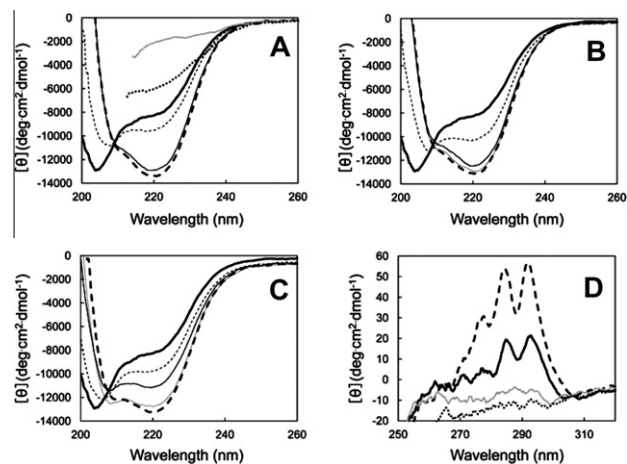
Fig. 2. CD spectra of Halo-RNH1. (A) The far-UV CD spectra measured in the absence of divalent metal ions and the presence of 0 M (*solid thick line*), 0.5 M (*dashed thin line*), 2 M (*solid thin line*), or 3 M (*dashed thick line*) NaCl are shown in comparison with those of Halo-RNH1 in a heat-denatured state (*dotted thick line*) and GdnHCl-denatured state (*gray thick line*). (B) The far-UV CD spectra measured in the absence of salt and the presence of 0 mM (*solid thick line*), 1 mM (*dashed thin line*), 5 mM (*solid thin line*), 10 mM (*dotted thin line*), or 20 mM (*dashed thick line*) MnCl$_2$ are shown. (C) The far-UV CD spectra measured in the absence of salt and the presence of 0 mM (*solid thick line*), 10 mM (*dashed thin line*), 50 mM (*solid thin line*), 300 mM (*dotted thin line*), or 500 mM (*dashed thick line*) MgCl$_2$ are shown. (D) The near-UV CD spectrum measured in the absence of salt and divalent metal ions (*solid thick line*) is shown in comparison with those of Halo-RNH1 in a native state (*dashed thick line*), heat-denatured state (*dotted thick line*), and GdnHCl-denatured state (*gray thick line*). These spectra were measured at 25 °C and pH 8.0, except for those in a heat-denatured state. The spectra of Halo-RNH1 in a native state, heat-denatured state, and GdnHCl-denatured state were measured at 25 °C and pH 8.0 in the presence of 3 M NaCl (native state) or 6 M GdnHCl (GdnHCl-denatured state), or 100 °C and pH 8.0 in the presence of 3 M NaCl (heat-denatured state), as described in Section 2.3.

of 2 M KCl or 200 mM CaCl$_2$ (data not shown). These results indicate that Halo-RNH1 requires either high concentrations of salt or moderate concentrations of divalent metal ions for folding. In contrast, *E. coli* RNase H1 requires neither salt nor divalent metal ions for folding [39]. Its spectrum is not significantly changed even in the presence of 2.5 M NaCl [40], suggesting that its structure is not significantly changed in a high-salt condition.

To examine whether Halo-RNH1 is partially folded or almost fully unfolded in the absence of salt and divalent metal ions, the far- and near-UV CD spectra of Halo-RNH1 were measured in the presence of 3 M NaCl at 100 °C (for heat-denatured state) or in the absence of salt and divalent metal ions and presence of 6 M GdnHCl at 25 °C (for GdnHCl-denatured state). The far-UV CD spectra of Halo-RNH1 were not measured at ≤210 nm in these conditions due to striking spectral fluctuation. As shown in Fig. 2(A), the far-UV CD spectrum of Halo-RNH1 without salt and divalent metal ions was different from those of Halo-RNH1 in a heat-denatured and GdnHCl-denatured state. The depth of a trough (or shoulder) in the former spectrum was deeper than those in the latter spectra. Likewise, the near-UV CD spectrum of Halo-RNH1 without salt and divalent metal ions, which reflects the environment of the tryptophan and tyrosine residues, was different from those of Halo-RNH1 in a heat-denatured and GdnHCl-denatured state, as shown in Fig. 2(D). The near-UV CD spectrum of Halo-RNH1 in a native state gave three peaks with [θ] values of 30 at 275 nm, 50 at 285 nm, and 55 at 295 nm. The spectrum of Halo-RNH1 without salt and divalent metal ions also gave these peaks but with much lower [θ] values. These peaks almost fully disappeared in the spectra of Halo-RNH1 in a heat-denatured and GdnHCl-denatured state. These results suggest that Halo-RNH1 is partially folded in the absence of salt and divalent metal ions.

Therefore, we define the structure of Halo-RNH1 in the absence of salt and divalent metal ions as a partially folded state (intermediate state) and that in the presence of salt or divalent metal ions as a folded state (native state), and designate Halo-RNH1s in an intermediate and native state as Halo-RNH1^I and Halo-RNH1^N, respectively. Halo-RNH1^I and Halo-RNH1^N change their conformations in a reversible manner. The far-UV CD spectra of Halo-RNH1 in the presence of 0.5 M NaCl (Fig. 2(A)), 1 mM MnCl$_2$ (Fig. 2(B)), and 10–50 mM MgCl$_2$ (Fig. 2(C)) suggest that these concentrations of salt and divalent metal ions are not sufficient to shift an equilibrium between Halo-RNH1^I and Halo-RNH1^N so that the fraction of Halo-RNH1^N increases to nearly 100%.

3.3. Protein stability

To examine whether salt and divalent metal ions affect the stability of Halo-RNH1^N, thermal denaturation of Halo-RNH1 was analyzed in the presence of divalent metal ions (20 mM MnCl$_2$ or 300 mM MgCl$_2$), salt (3 M NaCl), or both of them (20 mM MnCl$_2$ or 300 mM MgCl$_2$ and 3 M NaCl) by CD spectroscopy. Thermal denaturation of Halo-RNH1 was reversible and followed a two-state mechanism in these conditions. The results are shown in Fig. 3. The T_m values of Halo-RNH1 determined in these conditions are summarized in Table 1. The thermal denaturation curves in the presence of the Mn^{2+} ions are not shown in Fig. 3, because they were nearly identical to those in the presence of the Mg^{2+} ions. The T_m value of Halo-RNH1 determined in the presence of both divalent metal ions and salt is higher than those determined in the presence of divalent metal ions alone and salt alone by 26–30 °C and 9–10 °C, respectively, suggesting that salt and divalent metal ions independently contribute to the stabilization of Halo-RNH1^N by 26–30 °C and 9–10 °C, respectively.

It has been reported that *E. coli* RNase H1 is stabilized by approximately 10 °C in the presence of 2 mM MnCl$_2$, 50 mM CaCl$_2$, or 100 mM MgCl$_2$, and 17 °C in the presence of 2.5 M NaCl [40]. The stabilization effects of the divalent metal ions and NaCl are roughly additive. Divalent metal ions stabilize the protein by binding to the active site and suppressing negative charge repulsions at this site. Salt stabilizes the protein by increasing hydrophobic interactions at the protein core. Thus, the stabilization mechanisms of Halo-RNH1 with salt and divalent metal ions are similar to those of *E. coli* RNase H1, except that salt stabilizes Halo-RNH1 not only by increasing hydrophobic interactions at the protein core but also
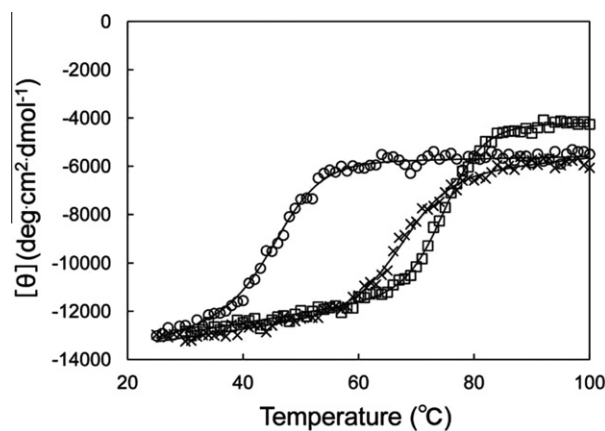

Fig. 3. Thermal denaturation curves of Halo-RNH1. The thermal denaturation curves of Halo-RNH1 measured in the presence of 300 mM MgCl$_2$ (*circle*), 3 M NaCl (*cross*), or 300 mM MgCl$_2$ and 3 M NaCl (*square*) are shown. These curves were obtained at pH 8.0 by monitoring the change in CD values at 222 nm at a scan rate of 1 °C/min, as described in Section 2.4. The theoretical curves are drawn on the assumption that the proteins are denatured via a two-state mechanism.

Table 1
T_m values of Halo-RNH1 and its derivatives.[a]

Protein	Metal	Salt	T_m (°C)	ΔT_m[b] (°C)
Halo-RNH1	300 mM MgCl$_2$		46.2 ± 0.1	–
	20 mM MnCl$_2$		50.0 ± 0.1	+3.8
		3 M NaCl	66.9 ± 0.1	+20.7
	300 mM MgCl$_2$	3 M NaCl	76.5 ± 0.1	+30.3
	20 mM MnCl$_2$	3 M NaCl	76.0 ± 0.1	+29.8
Halo-CTD	300 mM MgCl$_2$		45.7 ± 0.1	−0.5
	20 mM MnCl$_2$		53.8 ± 0.1	+7.6
		3 M NaCl	66.6 ± 0.1	+20.4
	300 mM MgCl$_2$	3 M NaCl	79.5 ± 0.1	+33.3
	20 mM MnCl$_2$	3 M NaCl	83.8 ± 0.1	+37.6
Halo-NTD		50 mM NaCl	44.6 ± 0.2	−1.6
		3 M NaCl	81.8 ± 0.1	+35.6

[a] The melting temperature (T_m), which is the temperature of the midpoint of the thermal denaturation transition, was determined from the thermal denaturation curve. The thermal denaturation curves of Halo-RNH1 in the presence of 300 mM MgCl$_2$, 3 M NaCl, or 300 mM MgCl$_2$ and 3 M NaCl are shown in Fig. 3 as representatives. Errors represent those for the fitting of the curves.

[b] ΔT_m is calculated as T_m of Halo-RNH1 or its derivative determined – T_m of Halo-RNH1 determined in the presence of 300 mM MgCl$_2$.
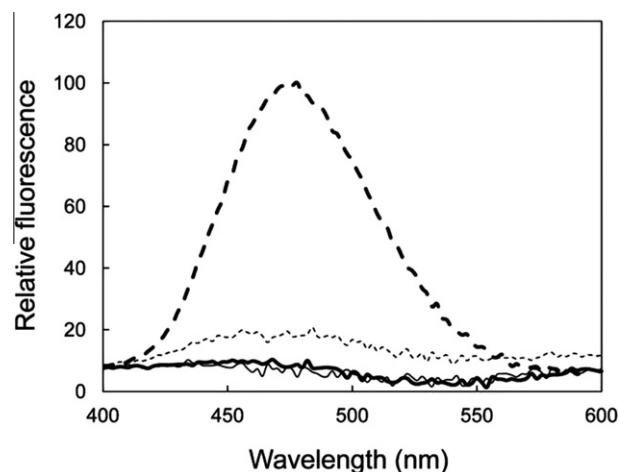

Fig. 4. ANS fluorescence spectra. The ANS fluorescence spectra of Halo-RNH1 was measured at 20 °C and pH 8.0 in the absence (*solid thick line*) or the presence of 20 mM MnCl$_2$ (*dashed thin line*), 3 M NaCl (*dashed thick line*), or 6 M GdnHCl (*solid thin line*), as described in Section 2.5.

by decreasing negative charge repulsions on the protein surface. Halo-RNH1 seems to be more significantly stabilized by salt than is *E. coli* RNase H1, probably because electrostatic repulsions on the protein surface of Halo-RNH1 are stronger than those of *E. coli* RNase H1.

Halo-RNH1[I] is incompletely folded probably because it is too unstable to be folded in the absence of salt and divalent metal ions. The finding that Halo-RNH1 is folded in the presence of 20 mM MnCl$_2$ and absence of salt suggests that negative charge repulsions at the active site are major forces that prevent folding of Halo-RNH1 in the absence of divalent metal ions and salt. Suppression of negative charge repulsions at the active site by binding of divalent metal ion(s) may be sufficient to facilitate folding of Halo-RNH1.

3.4. ANS fluorescence spectroscopy

To examine whether 1-anilino-8-naphthalenesulfonic acid (ANS) binds more effectively to Halo-RNH1 in a partially folded state than to that in a fully folded or unfolded state, as reported for non-halophilic proteins [41], ANS binding to Halo-RNH1 was analyzed in the presence or absence of salt (3 M NaCl), divalent metal ions (20 mM MnCl$_2$), or 6 M GdnHCl, by measuring the fluorescence spectrum of ANS. ANS becomes highly-fluorescent when it binds to a hydrophobic pocket of proteins [41]. As shown in Fig. 4, Halo-RNH1 exhibits ANS fluorescence in the presence of salt. However, it exhibits little ANS fluorescence in the presence of divalent metal ions, suggesting that ANS does not bind to Halo-RNH1[N]. It binds to Halo-RNH1[N] in the presence of salt, probably due to an increase in hydrophobicity on the protein surface. Halo-RNH1 exhibits little ANS fluorescence either in the absence of salt and divalent metal ions or in the presence of 6 M GdnHCl, suggesting that ANS binds to neither Halo-RNH1[I] nor Halo-RNH1 in an unfolded state. The high content of acidic residues on the protein surface may prevent the exposure of hydrophobic pockets in a partially folded state. It is also possible that hydrophobic pockets do not exist in a partially folded state of halophilic proteins.

3.5. Enzymatic activity

The enzymatic activity of Halo-RNH1 was determined in the presence of 50 mM or 3 M NaCl at 37 °C using the R12/D12 substrate. The concentration of MnCl$_2$ or MgCl$_2$ varied from 1 to 100 mM. *E. coli* RNase H1 did not exhibit activity in the presence of 3

M NaCl (data not shown). The separation of oligoribonucleotides produced upon hydrolysis of the substrate in the presence of 50 mM or 3 M NaCl on a urea gel is shown in Fig. 5. Halo-RNH1 cleaved the substrate at all sites between a4 and g11 with similar efficiencies in the presence of the Mn^{2+} ions regardless of the presence of 50 mM or 3 M NaCl. Likewise, it cleaved the substrate at four sites between a6 and c10, preferably at a6–u7 and a9–c10, in the presence of the Mg^{2+} ions regardless of the presence of 50 mM or 3 M NaCl. These results indicate that the cleavage-site specificity of Halo-RNH1, which varies for different divalent metal ions, is not seriously changed regardless of the presence of 50 mM or 3 M NaCl. However, the optimum concentration of divalent metal ions for activity in the presence of 3 M NaCl (1 mM for MnCl$_2$ or 20 mM for MgCl$_2$) was lower than that in the presence of 50 mM NaCl (20 mM for MnCl$_2$ or 100 mM for MgCl$_2$). The latter concentration is similar to that reported previously [25]. In a high-salt condition, in which Halo-RNH1 is folded, a physiological concentration of divalent metal ions seems to be sufficient to permit their binding to the active site and thereby to activate the enzyme. In contrast, in a low-salt condition, in which Halo-RNH1 is incompletely folded, higher concentrations of divalent metal ions are necessary to permit their binding to the active site and thereby to facilitate folding of the enzyme prior to the activation. Thus, divalent metal ions play a dual role in catalysis and folding of Halo-RNH1.

3.6. Binding to substrate

Binding of Halo-RNH1 to 29 bp RNA/DNA hybrid (R29/D29) was analyzed at 25 °C and pH 8.0 in the absence of divalent metal ions and presence of 50 mM or 3 M NaCl using surface plasmon resonance. Binding of *E. coli* RNase H1 to this substrate was also analyzed for comparative purposes. The protein was injected onto a sensor chip on which the R29/D29 substrate was immobilized. Halo-RNH1 did not bind to the substrate in the presence of 50 mM NaCl because it is not folded in a low-salt condition, but bound to it in the presence of 3 M NaCl. In contrast, *E. coli* RNase H1 bound to the substrate in the presence of 50 mM NaCl, but did not bind to it in the presence of 3 M NaCl. This is the reason why *E. coli* RNase H1 does not exhibit activity in the presence of 3 M NaCl. The association constant, K_A, of Halo-RNH1 was estimated to be 4.0×10^6 M^{-1} from the equilibrium binding level to the substrate in the presence of 3 M NaCl, while that of *E. coli* RNase H1 was estimated
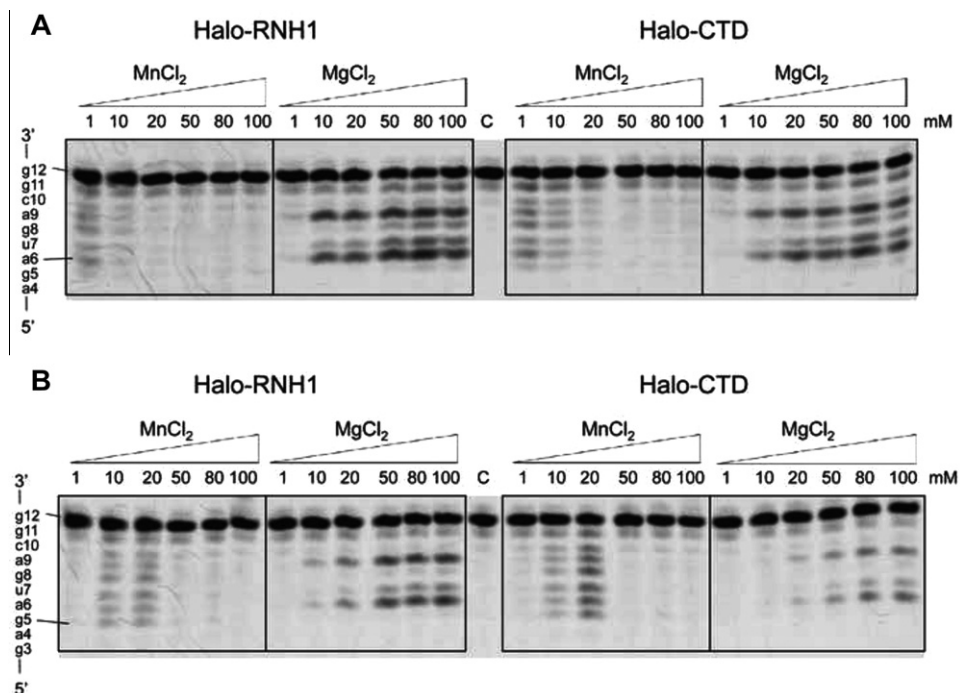
Fig. 5. Cleavage of the R12/D12 substrate with Halo-RNH1 and Halo-CTD. The 5′-end labeled R12/D12 substrate was hydrolyzed by Halo-RNH1 or Halo-CTD at 37 °C for 15 min in the presence of various concentrations of MnCl₂ or MgCl₂ and 3 M (A) or 50 mM (B) NaCl. The hydrolysates were separated on a 20% polyacrylamide gel containing 7 M urea. The concentration of the substrate was 1 μM. The amount of the enzyme added to the reaction mixture (10 μl) was 1 ng. The enzyme and divalent metal ions used to hydrolyze the substrate are shown above the gel together with the concentrations of the divalent metal ions. The sequence of R12 is indicated along the gel.

to be $2.7 \times 10^7 \, M^{-1}$ in the presence of 50 mM NaCl, which is comparable to that previously determined using the R36/D36 substrate ($4.7 \times 10^7 \, M^{-1}$) [42]. Thus, the K_A value of Halo-RNH1 is lower than that of *E. coli* RNase H1 by 8-fold, but is comparable to that of *Thermotoga maritima* RNase H1, which has been determined to be $6.3 \times 10^6 \, M^{-1}$ at pH 8.0 in the presence of 50 mM NaCl using the same substrate [32]. Like *E. coli* RNase H1, *T. maritima* RNase H1 loses the ability to bind to the substrate at high ($\geq$0.5 M) NaCl concentrations [32].

According to the co-crystal structures of *Bacillus halodurans* RNase H1 [9] and human RNase H1 [12] with the substrate, the RNA/DNA hybrid binds to the protein, in such a way that the RNA backbone fits in one groove containing the active site and the DNA backbone fits in the other groove. At the RNA-binding groove, the 2′-OH groups of four or five consecutive ribonucleotides form hydrogen bonds with the backbone atoms of the protein. At the DNA-binding groove, several polar residues form a phosphate-binding pocket, which is responsible for anchoring of the B-form DNA. High similarity of a tertiary model of Halo-RNH1 to that of *T. maritima* RNase H1 and the crystal structures of *E. coli* RNase H1, *B. halodurans* RNase H1, and human RNase H1 strongly suggests that the RNA/DNA hybrid binds to Halo-RNH1 in a similar manner. The binding affinity of Halo-RNH1 is lower than that of *E. coli* RNase H1 but is comparable to that of *T. maritima* RNase H1, probably because *E. coli* RNase H1 contains a basic protrusion whereas Halo-RNH1 and *T. maritima* RNase H1 do not. Electrostatic interactions between the basic protrusion and substrate have been reported to be important for substrate binding [42,43], more precisely for initial contact with the substrate [12]. In a high-salt condition, these electrostatic interactions may be suppressed and therefore the binding affinity of *E. coli* RNase H1 is greatly reduced. The reason why *E. coli* RNase H1 and *T. maritima* RNase H1 almost fully lose their binding ability to the substrate in a high-salt condition remains to be clarified. However, the strengthened binding ability of Halo-RNase H1 at

high salt concentration can be due to the ion uptake theory proposed by Bergqvist et al. [44]. While non-halophilic enzymes release ions (mainly cations) upon binding to the negatively charged DNA, binding of halophilic enzymes is characterized by the uptake of cations abundant in the medium as they are approaching the DNA, where these cations form a bridge between the DNA phosphate backbone and the negatively charged regions on the protein surface [45]. Alternatively, the conformation of the substrate may be changed in a high-salt condition, in such a way that the RNA and DNA backbones of the substrate do not fit in two grooves on the protein surface of non-halophilic enzymes but fit in those of halophilic enzymes.

3.7. Preparation of Halo-NTD and Halo-CTD

To analyze the role of an N-terminal domain of Halo-RNH1, Halo-NTD (residues 1–68) and Halo-CTD (residues 69–199) were constructed. Halo-NTD and Halo-CTD with the calculated molecular masses of 6975 and 14,023 Da, respectively, were overproduced in *E. coli* in a soluble form and purified to give a single band on SDS–PAGE (Fig. 6). The amount of the protein purified from 1 l of culture was typically 15 mg for both Halo-NTD and Halo-CTD. It has previously been reported that it is not possible to overproduce the Halo-RNH1 derivative without the N-terminal 60 residues in *E. coli* [25]. An eight-residue extension at the N-terminus of Halo-CTD may somehow prevent the production of the protein in *E. coli* cells.

3.8. Biochemical properties of Halo-NTD and Halo-CTD

The far-UV CD spectra of Halo-NTD and Halo-CTD indicate that Halo-NTD is folded regardless of the presence or absence of salt, whereas Halo-CTD is folded in a salt-dependent manner (Fig. 7). Halo-CTD is partially folded into an intermediate state in the absence of salt, but is folded into a native state in the presence of 2
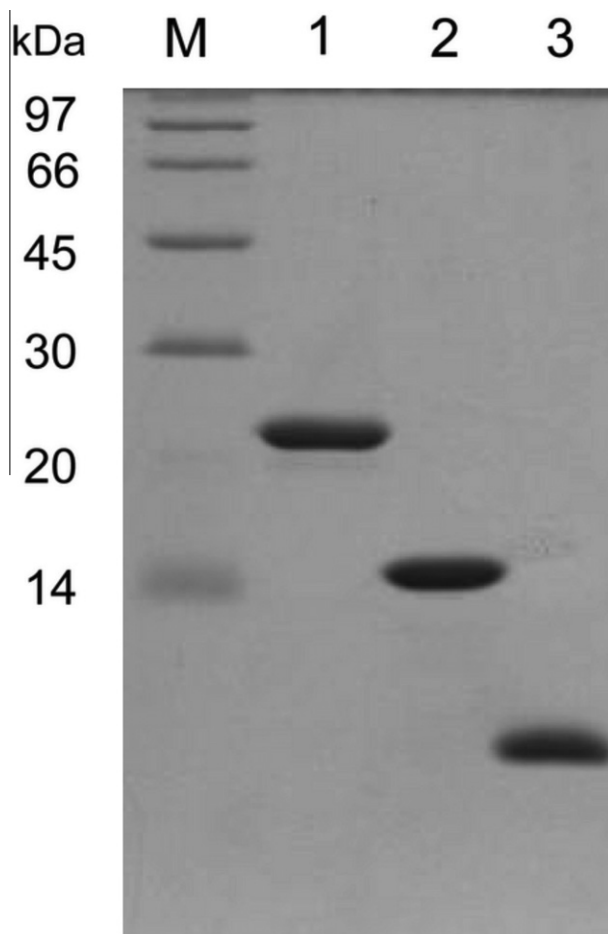
Fig. 6. Tricine SDS–PAGE of Halo-RNH1 and its derivatives. The purified proteins of Halo-RNH1 (lane 1), Halo-CTD (lane 2), and Halo-NTD (lane 3) were subjected to electrophoresis on a 15% polyacrylamide gel in the presence of SDS. After electrophoresis, the gel was stained with Coomassie Brilliant Blue. Lane M, a low-molecular-weight marker kit (GE Healthcare).

Fig. 7. Far-UV CD spectra of Halo-NTD and Halo-CTD. The spectra of Halo-NTD (A) and Halo-CTD (B) measured in the absence (*solid thick line*) or the presence of 0.5 M (*dashed thin line*), 2 M (*solid thin line*), or 3 M (*dashed thick line*) NaCl are shown. The spectra were measured at 25 °C and pH 8.0, as described in Section 2.3.

Table 2
Association constants of the proteins for substrate binding. [a]

Protein	K_A (M^{-1}) x 10^{-6}	Relative K_A[b]
Halo-RNH1	4.0	1.0
Halo-CTD	1.0	0.25
Halo-NTD	0.022	0.0055

[a] Binding of the proteins to 29 bp RNA/DNA hybrid immobilized onto the sensor chip was analyzed in the presence of 3 M NaCl and absence of divalent metal ions by surface plasmon resonance.
[b] The K_A value of the protein relative to that of Halo-RNH1.

M NaCl, as is the intact protein. Likewise, in the absence of salt, Halo-NTD is folded regardless of the presence or absence of divalent metal ions, whereas Halo-CTD is folded in a divalent metal ion-dependent manner (data not shown). Halo-CTD is fully folded in the presence of 10 mM MnCl$_2$ or 300 mM MgCl$_2$, as is the intact protein. Therefore, there is no significant difference in the folding behavior between Halo-CTD and the intact protein.

Halo-NTD and Halo-CTD are thermally denatured with a single transition in a reversible manner at the conditions examined as is the intact protein, as revealed by CD spectroscopy (data not shown). The T_m values of Halo-NTD determined in the presence of 50 mM or 3 M NaCl and those of Halo-CTD determined in the presence of divalent metal ions (20 mM MnCl$_2$ or 300 mM MgCl$_2$) and/or salt (3 M NaCl) are summarized in Table 1. Comparison of the T_m values of Halo-CTD suggests that salt and divalent metal ions independently contribute to the stabilization of Halo-CTD, but more significantly than to the stabilization of the intact protein, by 30–34 °C and 12–17 °C, respectively. The reason why salt and divalent metal ions more significantly contribute to the stabilization of Halo-CTD than to that of the intact protein remains to be clarified. Like Halo-CTD and the intact protein, Halo-NTD is greatly stabilized by 3 M NaCl by 35 °C, probably due to an increase in hydrophobic interactions at the protein core and a decrease in negative charge repulsions on the protein surface.

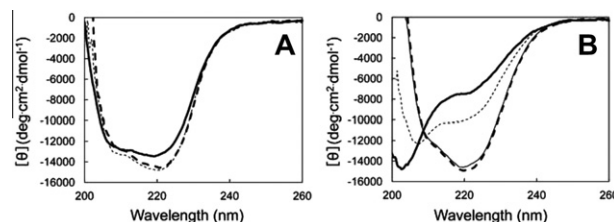Halo-CTD cleaved the R12/D12 substrate with similar cleavage site specificity to that of the intact protein either in the presence of MnCl$_2$ or MgCl$_2$ (Fig. 5). The optimum concentrations of MnCl$_2$ and MgCl$_2$ for activity of Halo-CTD are similar to those of the intact protein. The specific activities of Halo-CTD determined in the presence of 10 mM MnCl$_2$, 100 mM MgCl$_2$, and 50 mM or 3 M NaCl, which are nearly identical with one another, highly resemble those of the intact proteins (data not shown). The K_A value of Halo-CTD determined in the presence of 3 M NaCl and absence of divalent metal ions by surface plasmon resonance using the R29/D29 substrate is lower than that of the intact protein, but only by 4-fold (Table 2). In contrast, the K_A value of Halo-NTD is lower than that of the intact protein by 180-fold.

The results mentioned above thus indicate that an N-terminal domain of Halo-RNH1 is dispensable for stability, activity, folding, and substrate binding. It may possess an *in vivo* function that cannot be detected otherwise.

4. Conclusion

In this study, we showed that divalent metal ions play a dual role in catalysis and folding of *Halobacterium* sp. NRC-1 RNase H1 (Halo-RNH1). In a low-salt condition, Halo-RNH1 requires divalent metal ions not only for activity but also for folding. In a high-salt condition, Halo-RNH1 requires them only for activity. Divalent metal ions stabilize a native structure of Halo-RNH1 by binding to the active site and suppressing negative charge repulsions at this site. Salt stabilizes a native state of Halo-RNH1 by increasing hydrophobic interactions at the protein core and decreasing negative charge repulsions on the protein surface. Halo-RNH1 is incompletely folded in the absence of salt and divalent metal ions due to its great instability. In contrast, *E. coli* RNase H1 is fully folded in this condition. However, *E. coli* RNase H1 loses the binding ability to the substrate in a high-salt condition, probably due to a slight conformational change of the substrate binding site of the protein and/or the substrate. Halo-RNH1 may acquire the binding ability to the substrate in a high-salt condition by increasing the content of the acidic residues on the protein surface. Thus, Halo-RNH1 may lose the ability to fold in a low-salt condition at the cost of its functional adaptation to high-salt environment. Biochemical characterizations of the Halo-RNH1 derivatives without an N- or C-terminal

domain indicate that the N-terminal domain is dispensable for stability, activity, folding, and substrate binding.

Acknowledgement

References

[1] Lazzaro, F., Novarina, D., Amara, F., Watt, D.L., Stone, J.E., Costanzo, V., Burgers, P.M., Kunkel, T.A., Plevani, P. and Muzi-Falconi, M. (2012) RNase H and postreplication repair protect cells from ribonucleotides incorporated in DNA. Mol. Cell 45, 99–110.

[2] Itaya, M., Omori, A., Kanaya, S., Crouch, R.J., Tanaka, T. and Kondo, K. (1999) Isolation of RNase H genes that are essential for growth of *Bacillus subtilis* 168. J. Bacteriol. 181, 2118–2123.

[3] Cerritelli, S.M., Frolova, E.G., Feng, C., Grinberg, A., Love, P.E. and Crouch, R.J. (2003) Failure to produce mitochondrial DNA results in embryonic lethality in *Rnaseh1* null mice. Mol. Cell 11, 807–815.

[4] Schultz, S.J. and Champoux, J.J. (2008) RNase H activity: structure, specificity, and function in reverse transcription. Virus Res. 134, 86–103.

[5] Beilhartz, G.L. and Götte, M. (2010) HIV-1 Ribonuclease H: structure, catalytic mechanism and inhibitors. Viruses 2, 900–926.

[6] Ohtani, N., Haruki, M., Morikawa, M. and Kanaya, S. (1999) Molecular diversities of RNases H. J. Biosci. Bioeng. 88, 12–19.

[7] Crouch R.J., Dirksen M.L. (1982) Ribonuclease H. In Nuclease (S.M. Linn, R.J. Roberts, Eds.), Cold Spring Harbor, NY: Cold Spring Harbor Laboratory Press; pp. 211–241.

[8] Tadokoro, T. and Kanaya, S. (2009) Ribonuclease H: molecular diversities, substrate binding domains, and catalytic mechanism of the prokaryotic enzymes. FEBS J. 276, 1482–1493.

[9] Nowotny, M., Gaidamakov, S.A., Crouch, R.J. and Yang, W. (2005) Crystal structures of RNase H bound to an RNA/DNA hybrid: substrate specificity and metal-dependent catalysis. Cell 121, 1005–1016.

[10] Nowotny, M. and Yang, W. (2006) Stepwise analyses of metal ions in RNase H catalysis from substrate destabilization to product release. EMBO J. 25, 1924–1933.

[11] Yang, W., Lee, J.Y. and Nowotny, M. (2006) Making and breaking nucleic acids: two-Mg^{2+}-ion catalysis and substrate specificity. Mol. Cell 22, 5–13.

[12] Nowotny, M., Gaidamakov, S.A., Ghirlando, R., Cerritelli, S.M., Crouch, R.J. and Yang, W. (2007) Structure of human RNase H1 complexed with an RNA/DNA hybrid: insight into HIV reverse transcription. Mol. Cell 28, 264–276.

[13] Ng, W.V., Kennedy, S.P., Mahairas, G.G., Berquist, B., Pan, M. and Shukla, H.D. et al. (2000) Genome sequence of *Halobacterium* species NRC-1. Proc. Natl. Acad. Sci. USA 97, 12176–12181.

[14] Paul, S., Bag, S.K., Das, S., Harvill, E.T. and Dutta, C. (2008) Molecular signature of hypersaline adaptation: insights from genome and proteome composition of halophilic prokaryotes. Genome Biol. 9, R70.

[15] Elcock, A.H. and McCammon, J.A. (1998) Electrostatic contributions to the stability of halophilic proteins. J. Mol. Biol. 280, 731–748.

[16] Madern, D., Ebel, C. and Zaccai, G. (2000) Halophilic adaptation of enzymes. Extremophiles 4, 91–98.

[17] Mevarech, M., Frolow, F. and Gloss, L.M. (2000) Halophilic enzymes: proteins with a grain of salt. Biophys. Chem. 86, 155–164.

[18] Ishibashi, M., Tokunaga, H., Hiratsuka, K., Yonezawa, Y., Tsurumaru, H., Arakawa, T. and Tokunaga, M. (2001) NaCl-activated nucleoside diphosphate kinase from extremely halophilic archaeon, *Halobacterium salinarum*, maintains native conformation without salt. FEBS Lett. 493, 134–138.

[19] Arakawa, T. and Tokunaga, M. (2004) Electrostatic and hydrophobic interactions play a major role in the stability and refolding of halophilic proteins. Protein Pept. Lett. 11, 125–132.

[20] Besir, H., Zeth, K., Bracher, A., Heider, U., Ishibashi, M., Tokunaga, M. and Oesterhelt, D. (2005) Structure of a halophilic nucleoside diphosphate kinase from *Halobacterium salinarum*. FEBS Lett. 579, 6595–6600.

[21] Wright, D.B., Banks, D.D., Lohman, J.R., Hilsenbeck, J.L. and Gloss, L.M. (2002) The effect of salts on the activity and stability of *Escherichia coli* and *Haloferax volcanii* dihydrofolate reductases. J. Mol. Biol. 323, 327–344.

[22] Gloss, L.M., Topping, T.B., Binder, A.K. and Lohman, J.R. (2008) Kinetic folding of *Haloferax volcanii* and *Escherichia coli* dihydrofolate reductases: haloadaptation by unfolded state destabilization at high ionic strength. J. Mol. Biol. 376, 1451–1462.

[23] Bandyopadhyay, A.K., Krishnamoorthy, G., Padhy, L.C. and Sonawat, H.M. (2007) Kinetics of salt-dependent unfolding of [2Fe–2S] ferredoxin of *Halobacterium salinarum*. Extremophiles 11, 615–625.

[24] Coquelle, N., Talon, R., Juers, D.H., Girard, E., Kahn, R. and Madern, D. (2010) Gradual adaptive changes of a protein facing high salt concentrations. J. Mol. Biol. 404, 493–505.

[25] Ohtani, N., Yanagawa, H., Tomita, M. and Itaya, M. (2004) Identification of the first archaeal Type 1 RNase H gene from *Halobacterium* sp. NRC-1: archaeal RNase HI can cleave an RNA-DNA junction. Biochem. J. 381, 795–802.

[26] Kanaya, S. and Crouch, R.J. (1983) DNA sequence of the gene coding for *Escherichia coli* ribonuclease H. J. Biol. Chem. 258, 1276–1281.

[27] Kanaya, S., Oobatake, M., Nakamura, H. and Ikehara, M. (1993) pH-dependent thermostabilization of *Escherichia coli* ribonuclease HI by histidine to alanine substitutions. J. Biotechnol. 28, 117–136.

[28] Schägger, H. (2006) Tricine–SDS–PAGE. Nat. Protoc. 1, 16–22.

[29] Kanaya, S., Kimura, S., Katsuda, C. and Ikehara, M. (1990) Role of cysteine residues in ribonuclease H from *Escherichia coli*. Site-directed mutagenesis and chemical modification. Biochem. J. 271, 59–66.

[30] Goodwin, T.W. and Morton, R.A. (1946) The spectrophotometric determination of tyrosine and tryptophan in proteins. Biochem. J. 40, 628–632.

[31] Ohtani, N., Haruki, M., Morikawa, M., Crouch, R.J., Itaya, M. and Kanaya, S. (1999) Identification of the genes encoding Mn^{2+}-dependent RNase HII and Mg^{2+}-dependent RNase HIII from *Bacillus subtilis*: classification of RNases H into three families. Biochemistry 38, 605–618.

[32] Jongruja, N., You, D.J., Kanaya, E., Koga, Y., Takano, K. and Kanaya, S. (2010) The N-terminal hybrid binding domain of RNase HI from *Thermotoga maritima* is important for substrate binding and Mg^{2+}-dependent activity. FEBS J. 277, 4474–4489.

[33] Schwede, T., Kopp, J., Guex, N. and Peitsch, M.C. (2003) SWISS-MODEL: an automated protein homology-modeling server. Nucl. Acids Res. 31, 3381–3385.

[34] Watkins, H.A. and Baker, E.N. (2010) Structural and functional characterization of an RNase HI domain from the bifunctional protein Rv2228c from *Mycobacterium tuberculosis*. J. Bacteriol. 192, 2878–2886.

[35] Baker, N.A., Sept, D., Joseph, S., Holst, M.J. and McCammon, J.A. (2001) Electrostatics of nanosystems: application to microtubules and the ribosome. Proc. Natl. Acad. Sci. USA 98, 10037–10041.

[36] Katayanagi, K., Okumura, M. and Morikawa, K. (1993) Crystal structure of *Escherichia coli* RNase HI in complex with Mg^{2+} at 2.8 A resolution: proof for a single Mg^{2+}-binding site. Proteins 17, 337–346.

[37] Goedken, E.R. and Marqusee, S. (2001) Co-crystal of *Escherichia coli* RNase HI with Mn^{2+} ions reveals two divalent metals bound in the active site. J. Biol. Chem. 276, 7266–7271.

[38] Tsunaka, Y., Takano, K., Matsumura, H., Yamagata, Y. and Kanaya, S. (2005) Identification of single Mn^{2+} binding sites required for activation of the mutant proteins of *E. coli* RNase HI at Glu48 and/or Asp134 by X-ray crystallography. J. Mol. Biol. 345, 1171–1183.

[39] Kanaya S. (1998) Enzymatic activity and protein stability of *E.coli* ribonuclease HI In Ribonucleases H (R.J. Crouch, J.J. Toulmé, Eds.), Paris: INSERM; pp. 1–38.

[40] Kanaya, S., Oobatake, M. and Liu, Y. (1996) Thermal stability of *Escherichia coli* ribonuclease HI and its active site mutants in the presence and absence of the Mg^{2+} ion. Proposal of a novel catalytic role for Glu48. J. Biol. Chem. 271, 32729–32736.

[41] Kuwajima, K. (1989) The molten globule state as a clue for understanding the folding and cooperativity of globular-protein structure. Proteins 6, 87–103.

[42] Haruki, M., Noguchi, E., Kanaya, S. and Crouch, R.J. (1997) Kinetic and stoichiometric analysis for the binding of *Escherichia coli* ribonuclease HI to RNA–DNA hybrids using surface plasmon resonance. J. Biol. Chem. 272, 22015–22022.

[43] Kanaya, S., Katsuda-Nakai, C. and Ikehara, M. (1991) Importance of the positive charge cluster in *Escherichia coli* ribonuclease HI for the effective binding of the substrate. J. Biol. Chem. 266, 11621–11627.

[44] Bergqvist, S., Williams, M.A., O'Brien, R. and Ladbury, J.E. (2003) Halophilic adaptation of protein–DNA interactions. Biochem. Soc. Trans. 31, 677–680.

[45] O'Brien, R., DeDecker, B., Fleming, K.G., Sigler, P.B. and Ladbury, J.E. (1998) The effects of salt on the TATA binding protein–DNA interaction from a hyperthermophilic archaeon. J. Mol. Biol. 279, 117–125.